HHS Public Access

Author manuscript

Ann Biomed Eng. Author manuscript; available in PMC 2020 January 01.

Published in final edited form as:

Ann Biomed Eng. 2019 January ; 47(1): 75–84. doi:10.1007/s10439-018-02120-0.

Sinus Hemodynamics Variation with Tilted Transcatheter Aortic Valve Deployments

Hoda Hatoum, MS[1], **Jennifer Dollery, RN**[2], **Scott M. Lilly, MD, PhD**[3], **Juan A. Crestanello, MD**[2], and **Lakshmi Prasad Dasi, PhD**[1,2]

[1]Department of biomedical engineering, The Ohio State University, Columbus, Ohio, USA

[2]Division of cardiac surgery, The Ohio State University, Columbus, Ohio, USA

[3]Division of cardiovascular medicine, The Ohio State University, Columbus, Ohio, USA

Abstract

Leaflet thrombosis is a complication associated with transcatheter aortic valve(TAV) replacement(TAVR) correlated with sinus flow stasis. Sinus hemodynamics are important because they dictate shear stress and washout necessary to avoid stasis on TAV leaflets. Sinus flow is controlled by TAV axial deployment position but little is known regarding TAV axis misalignment effect. This study aims to elucidate TAV angular misalignment with respect to aortic root axis effect on sinus flow stasis potentially leading to leaflet thrombosis. Sinus hemodynamics were assessed *in-vitro* using particle-image velocimetry in three different angular misalignments with respect to aorta axis: untilted, tilted away from the sinus and tilted towards sinus. A 26mm Edwards SAPIEN3 was implanted in a 3D printed model of an anatomically realistic aortic root. TAV hemodynamics, sinus vortex tracking, leaflet shear stress probability density functions, and sinus blood time to washout were calculated. While pressure gradients differed insignificantly, blood velocity and vorticity decreased significantly in both tilted cases sinuses. Shear stress probability near the leaflet decreases with tilt indicating stasis. TAV tilted away from the sinus is the most unfavorable scenario with poor washout. TAV axial misalignment adds to factors list that could influence leaflet thrombosis risk through modifying sinus hemodynamics and washout.

Keywords

Transcatheter aortic valves; TAVR; axial tilt; sinus hemodynamics; thrombosis; particle image velocimetry; sinus flows; TAV misalignment; sinus washout.

Introduction

Transcatheter aortic valve (TAV) replacement (TAVR) is a non-invasive procedure relevant to patients who are classified as high-risk patients for traditional open heart surgery[1].

Address for correspondence and reprints: Lakshmi Prasad Dasi, PhD, Associate Professor, Department of Biomedical Engineering, The Ohio State University 473 W 12th Ave., Columbus, OH 43210, TEL: (614) 247-8313, lakshmi.dasi@osumc.edu.

Conflict of Interest: Dr. Dasi reports having a patent application filed on novel polymeric valves, vortex generators and and superhydrophobic/superomniphobic heart valves and Dr. Crestanello reports having grants from Medtronic, Boston Scientific and Abbot in addition to being part of the advisory board for Medtronic. No other conflicts were reported.

Adverse effects such as elevated post-procedure pressure gradients, paravalvular leakage, coronary obstruction and recently sub-clinical leaflet thrombosis have been associated with TAVR[2–5]. Leaflet thrombosis in particular can be identified with Computed Tomography (CT) imaging[5, 6]. Many *in-vivo* clinical studies have tried to identify possible causes leading to leaflet thrombosis such as retention of blood flow and stasis in the sinuses and at the base of the leaflets[7–9], lower implants of TAVs[7, 8], under-expansion and asymmetry of the TAV[8], incomplete TAV apposition to the aortic wall[9, 10], the metallic frame of the TAV[9, 10] and other conditions.

In this *in-vitro* study, we examine another possible reason that may lead to the formation of leaflet thrombosis stemming for *in-vivo* patient cases. An 86 year-old man underwent TAVR and at an in-clinic evaluation 6 months later due to worsening dyspnea with exertion, a harsh systolic murmur was detected and an echocardiogram was performed. The results of the echo revealed flow acceleration with a mean pressure gradient (PG) of 52mmHg which was significantly higher than prior to discharge post-TAVR. The patient was receiving warfarin however this was discontinued due to recurrent gastrointestinal bleeding (GI). A CT scan revealed leaflet thrombus formation (Fig. 1A and B). Another 84 year old patient underwent TAVR and after 6 months went through the same symptoms described above. Thrombus was detected as shown in Fig. 1C and D. The *in-vivo* study by Makkar et al[6] showed some sample cases of CT scans for patients' valves with leaflet thrombosis (Fig. 1E, F, G and H). From Fig. 1, the TAVs implanted in these cases were tilted with respect to the axis of the aorta (yellow lines), bringing the question of the relative valve angulation and its potential influence on sinus flow stasis that's associated with leaflet thrombosis. The tilt angles are shown (Fig. 1B, D, F and H) and mark the difference between the aortic longitudinal axis and that of the TAV. For every section view, the corresponding top aortic view is shown (Fig. 1 A, C, E and G) with arrows pointing to the thrombus location. From a fluid dynamics argument alone tilting of the forward jet towards or away from the sinus can influence sinus vortex dynamics.

The objective of this study is to perform a controlled *in-vitro* experiment to study the effect of different axial tilt orientation of the TAV with respect to the axis of the aortic root on flow stasis as well as washout characteristics in the sinus in the context of better understanding the patho-mechanics of leaflet thrombosis.

Materials and Methods

In-vitro modelling

This study was approved by the institutional review board (IRB) and access to patient data was granted after the patients' consent was obtained as part of the study. The high spatial resolution of the Computed Tomography (CT) imaging data provide clear depiction of the aortic valve cusps and calcific regions.

Contrast enhanced CT DICOM images at the 85% phase were imported into anatomic modeling software (Mimics, Materialise, Belgium). The left ventricular outflow tract (LVOT), valve cusps, ascending aorta, and all calcified tissues were segmented individually and then reconstructed into a model consisting of 2 paired stereolithographic files composed

of the calcified and non-calcified structures within the data set. Fig. 2a and 2b show the aortic view and the sinus view respectively. These stereolithographic files were exported to a Stratasys Connex Printer where the files were used to create a fused material 3D construct of the predefined anatomic region. Cusp calcification was replicated using rigid print material (VeroWhite clear) and soft tissue structures, including the non-calcified cusp segments, LVOT, and ascending aorta, were replicated using a rubber-like material (TangoPlus FLX930). The model was coated externally with a thin layer of silicon to improve visual clarity and durability. Print material properties were chosen to best represent the complex tissue properties of an aortic root. The print material used for the non-calcified anatomic regions (TangoPlus) has a manufacturer-reported elastic modulus of 0.1 MPa at 20% strain and 0.2MPa at 30% strain. The print material used for the calcified anatomic region (VeroWhitePlus) has a manufacturer-reported elastic modulus of 2000 to 3000 MPa.

The valve native annulus area and perimeter at mid-systole were measured to be 366mm^2 and 69.1mm respectively. This patient's heart rate and cardiac output were 81bpm and 5.3L/min respectively.

The model was created based on the methodology of Maragiannis et al[11] and Hatoum et al[12, 13].

Valve selection and deployment

A 26mm Edwards SAPIEN 3 TAV was selected and implanted at 3 different angulations with the axis of the valve (1) in line with the axis of the aorta, (2) tilted away from the sinus (downwards with respect to the axis of the aorta) by a 12 degree angle and (3) tilted towards the sinus (upwards) by a 12 degree angle as shown in Fig. 2c and d. These tilt angle values fall within the range found in-vivo cases as shown in Fig. 1 and are defined as the angles between the longitudinal axis of the aorta and that of the TAV. The selection of the appropriate TAV size was based on the recommendations of Kasel et al[14]. A sketch of the valve axial tilt with respect to the axis of the aorta is shown in Fig. 2e.

Hemodynamic assessment

Hemodynamic parameters were evaluated under pulsatile flow conditions ensured by a left heart simulator yielding physiological flow and pressure curves[15, 16]. The desired outputs can be summarized as establishing a systolic to diastolic pressure of 120/80mmHg, an 81bpm heart rate, a systolic duration of 33% and a cardiac output of 5.3L/min. The working fluid in this study is a mixture of water-glycerine (99% pure glycerine) producing a density of 1080 Kg/m^3 and a kinematic viscosity of 3.5cSt similar to blood properties. Sixty consecutive cardiac cycles of aortic pressure, ventricular pressure and flow rate data were recorded at a sampling rate of 100Hz. The mean transvalvular pressure gradient (PG) is defined as the average of positive pressure difference between the ventricular and aortic pressure curves during forward flow.

Particle Image Velocimetry (PIV)

PIV was performed to capture high spatio-temporal resolution blood flow velocity fields and particle washout characteristics within the sinus for all cases. The flow was seeded with

fluorescent PMMA-Rhodamine B particles with diameters ranging from 1 to 20μm. The velocity field within the sinus region, including the region adjacent to the TAV leaflets, was measured using high spatial and temporal resolution PIV. Briefly, this involved illuminating the sinus region using a laser sheet created by pulsed Nd:YLF single cavity diode pumped solid state laser coupled with external spherical and cylindrical lenses; while acquiring high-speed images of the fluorescent particles within the sinus region. The laser was generated using the Photonics Industries DM40–527 diode-pump Q-switched laser (Photonics, Bohemia, NY) with optics to covert the output beam into an expanded laser sheet. The laser had an initial thickness of approximately 1 mm, which was focused down to less than 200 microns within the measurement region using a spherical lens (f = 1m). Raw PIV images were acquired with a resulting spatial and temporal resolutions of 0.02964mm/pixel and 4000Hz respectively. Refraction was corrected using a calibration in DaVis particle image velocimetry software (DaVis 7.2, LaVision Germany). Velocity vectors were calculated using adaptive cross-correlation algorithms. Further details of PIV measurements can be found in Hatoum et al[12, 13, 16–20].

Sinus Vorticity and Shear Stress Dynamics

Using the velocity measurements from PIV, vorticity dynamics (as previously done[16, 17, 21]) were also evaluated for the sinus region. Vorticity is the curl of the velocity field and therefore captures localized rotation of blood. Regions of high vorticity indicate both shear and rotation of the fluid particles. Vorticity was computed using the following equation:

$$\omega_z = -\left(\frac{dV_x}{dy} - \frac{dV_y}{dx}\right) \quad (1)$$

Where ω is the measured vorticity component with units of s^{-1}; V_x and V_y are the x and y components of the velocity vector with units of m/s. The x and y directions are axial and lateral respectively.

Viscous shear stress field was evaluated consistently with Hatoum et al[12, 13, 18, 19, 22, 23] and Moore et al[21].

$$\tau = \mu\left(\frac{dV_x}{dy} + \frac{dV_y}{dx}\right) \quad (2)$$

Where τ is the shear stress in Pascal (Pa) and μ is the dynamic viscosity in $N.s/m^2$.

Sinus washout

Velocity measurements from PIV were also used to evaluate sinus washout. Sinus washout is defined as the characteristic curve representing the percent of fluid particles, initially seeded in the sinus region at the beginning of the cardiac cycle, and still remaining in the sinus as a function of time plotted over the cardiac cycle. Ideally good washout is associated with a high percentage of particles exiting over a minimum number of cardiac cycles. To quantify

sinus washout curves, first particle tracking was performed similar to other studies [13, 22, 24–26]. Briefly, particles were seeded as a uniform grid of 1mm x 1mm cell size over the sinus region at the beginning of the cardiac cycle. Each particle's trajectory was computed by integrating its velocity with respect to time based on:

$$\frac{d\vec{x}}{dt}(t) = \vec{u}((\vec{x}), t)) \quad (3)$$

With:

$$\vec{x}(t = 0) = \vec{x}_0 \quad (4)$$

The integration time step was 0.00025s and at the end of every time step, the particle's velocity vector was calculated based on the particle's updated location through interpolating the PIV velocity data.

After every cardiac cycle only the particles that remained in the sinus were re-seeded based on their last positions and their trajectory over the subsequent cardiac cycle was calculated. This process continued until all particles exited or until 10 cardiac cycles elapsed because by 10 cycles no more significant particles exited the sinus from the initial seeding.

Once all the particles exited the sinus, a histogram of the time spent by the particles was generated and then converted to a cumulative distribution function representing the particles' survival probability as a function of time. This procedure is repeated over 10 cycles for every case. The resulting curves represent the sinus washout characteristic for all cases.

Results

a- Hemodynamic parameters

Table 1 summarizes some *in-vitro* hemodynamic parameters post-TAVR for the three cases. The average PG obtained with the untilted SAPIEN3 was 20.14±0.16mmHg, 17.71±0.77mmHg with the SAPIEN tilted away from the sinus and 15.32±0.33mmHg with the SAPIEN tilted towards the sinus. The pressure gradient obtained pre-TAVR was found to be 49.4mmHg.

b- Flow velocity fields

Fig. 3 shows the velocity vectors and vorticity contours within the sinus of the three different valve cases at selected time points throughout the cardiac cycle. Both velocity and vorticity patterns are different in the sinus with the different deployment types. Having a tilt in the axial orientation of the valve with respect to the axis of the aorta leads to different vortex propagation mechanisms during systole. Because of the different jet orientations, it is important to note that in the case of tilt away from the sinus, a clockwise (CW) vortex forms due to the large recirculation region evident near the sinotubular junction (STJ). While in the tilted towards sinus orientation case, the counterclockwise (CCW) vortex forms and interacts

with the sinus wall immediately and directly near the sinotubular junction side. The peak velocities within the sinus are found to be 0.34m/s, 0.13m/s and 0.20m/s in the untilted, tilted away from the sinus and tilted towards the sinus cases respectively. The peak vorticities are $250s^{-1}$, $91s^{-1}$ and $89s^{-1}$ in the untilted, tilted away from the sinus and tilted towards sinus cases respectively.

During diastole, the velocity in the sinus reaches 0.15m/s, 0.10m/s and 0.12m/s for the untilted SAPIEN, for the tilted away and towards the sinus respectively in mid-diastole.

c- Shear stress distribution

Figs. 4a and b show the probability density function (PDF) of flow shear stress magnitude in the region adjacent to the leaflets during systole and diastole, respectively. As is clearly evident in part a, higher peak shear stresses (up to 1.2Pa) occur when the SAPIEN is untilted however the likelihood of this peak shear stress decreases once a tilt whether towards or away from the sinus is introduced (only up to 0.6Pa). Having the tilt towards the sinus provides slightly higher shear stress probabilities near the leaflets compared with the one away from the sinus during systole. During diastole (Fig 4b), having the untilted SAPIEN still provides higher likelihood of developing higher peak shear stress values near the leaflets with shear stress almost reaching 1.0Pa. The tilts changed the diastolic shear stress probabilities by decreasing it compared to the untilted case. Nevertheless, during diastole having the tilt towards the sinus is almost comparable to the untilted case while the one with the away tilt shows smaller values (up to 0.6Pa).

d- Sinus washout

Fig. 5 shows the survival probability curve of particles remaining in the sinus for the three different valve cases. When the SAPIEN3 is tilted away from the sinus, 21% of the particles exit the sinus region (79% remain) after the first cardiac cycle, followed by an additional 39% at the end of the second cycle. The decrease in particle remaining is continuously slow throughout the cardiac cycles reaching a total washout after 9.5 cycles.

With the SAPIEN tilted towards the sinus, 88.32% of the particles exit (11.68% remain) the sinus after the first cardiac cycle, and total washout takes place at the end of the second cardiac cycle.

The untilted SAPIEN represents a midway case where 75% of the particles exit the sinus at the end of the first cardiac cycle then the decease becomes slow till total washout is achieved after 7.5 cycles.

Discussion

a- Hemodynamic parameters

The pressure gradients varied between the different deployment cases although the differences are clinically insignificant. Tilt can help with early re-attachment of the forward jet along the aortic wall that the jet impinges on and therefore better pressure recovery which may explain the minor improvement in pressure gradient with the tilts. Having the tilt may have also provided a bigger orifice area – because the SAPIEN stent is less constrained

during balloon inflation on the side that's not aligned with the axis of the aorta. The more the tilt, the more a portion of the stent is unconstrained leading to a potentially wider (albeit insignificant) opening.

b- Flow velocity fields

Introducing a tilt to the valve deployment with respect to the axis of the aortic root clearly modifies the sinus vortex propagation mechanism (shape, motion and stability) in the different valve cases due to the different relative orientations between the forward jet and the ascending aorta[27, 28].

Sinus flow patterns were altered decreasing sinus velocity, modifying the vortex formation and propagation mechanisms in the sinus, and increasing regions of flow stasis especially at the base of the sinus. The orientation of the SAPIEN with respect to the annulus has altered the direction of the flow. The vortex starts propagating in the sinus region later in the cardiac cycle for the tilted SAPIENs compared to the untilted case.

When the SAPIEN is implanted without tilt, a vortex starts forming at the leaflet tip and develops to get bigger and propagate inside the sinus as is clear at the peak phase providing fast mixing and rotation within the sinus[29]. This how normal sinus flow is established and relies on the vortex formation and entrapment into the sinus with the appropriate interaction with the sinus ridge at the STJ.

When the SAPIEN is tilted away from the sinus, as the leaflet opens and because of the tilt, the jet is correspondingly oriented downwards. The vortex that is formed at the edge of the leaflet now fails to propagate inside the sinus because sinus fluid is now more in the entrainment region of the forward jet thereby exiting the sinus rather than actually rotating there. As the leaflet closes and the pressure gradient reverses, vortices start forming driven by flow reversal and a mixing takes place. The overall motion in the sinus when the SAPIEN is tilted away from the sinus, becomes less about rotation and more about having the particles attempt to exit the region which shows that the main jet leads the flow from the back of the sinus.

When the SAPIEN is tilted towards the sinus, as the leaflet starts opening, the main jet itself, due to the orientation, impinges the STJ side leading to having the vortex, at the beginning near the tip of the leaflet, adjacent to the exit side of the sinus. The usual propagation and entrapment of vortex does not occur. This can be attributed to the higher dynamic pressure in the sinus with the jet pointed towards the sinus. The higher pressure in the sinus prevents any flow or vortexes into the sinus as compared to the untilted case where there is a dynamically favorable condition for the vortex to enter the sinus. As is clear at peak systole, the overall flow in the sinus tends to stagnate in the region than rotate there. Having it tilted towards the sinus leads to having the main flow hit the sinus edge adjacent to the STJ leading to having the vortex experience an impact with the wall leading to vortex stretching[30] at peak systole.

The two tilted orientations both lead to decreased blood flow motion near the leaflets compared to the untilted placement of the TAV with respect to the axis of the aortic root.

c- Shear stress distribution

Thrombosis is most likely to occur in low-flow or stasis regions with reduced shear stresses[2, 22, 31]. In healthy blood vessels, shear stress values range from 1.5 to 2Pa[13, 22, 32].Usually shear stress varies with the local conditions and the flow rate. Very low values of shear stress change the behavior of some cells for example platelets and can lead to thrombus formation[33]. It is the shear-dependent mass transport that is responsible for atheroma growth and thus higher risk of thrombosis. Furthermore, the endothelium has been shown to become atherogenic when exposed to low wall shear stress[33, 34]. Several studies have reported and classified shear stress values in grafts as “high” and “low”[35] and suggested low values of shear stress to be 0.25Pa and 0.31Pa while the high values were 1.54Pa and 1.71Pa. Another study of vascular shear stress by Cuningham et al[36] and Saw et al[37] showed that vascular shear stress of large conduit arteries typically varies between 5 and 20 dynes/cm^2 (0.5 to 2.0Pa). Another study by Casa et al[38] reported a normal value of 1000s^{-1} for shear rate that corresponds to 3.5Pa in arteries and a value of 500s^{-1} corresponding to 1.75Pa in coronary arteries. A study by Bark et al[38] has reported physiological arterial shear rates below 400s^{-1} equivalent to 1.4Pa. Having said this, high likelihood of high shear stress near the leaflet is desirable while lower likelihood of high shear stress is not favorable as low shear stress is associated with higher likelihoods of developing thrombus.

Despite the decreased high shear stress likelihood once a tilt is introduced, the one with the tilt towards sinus showed higher probabilities of high shear stress than the downward one. The reason may be that the flow still retains more momentum compared with when the jet is projected downwards thus having a greater influence on the particle flow inside the sinus[39]. This finding is confirmed by the vorticity and velocity patterns observed in the sinuses.

One of the reasons we observe the differences between diastole and systole, can be due to the additional space that the downward orientation provides for the backflow (unimpeded by the decelerating main jet) during pressure gradient reversal to enter the sinus. Having lower or higher shear stress levels near the leaflets of the valve in the sinus depending on the orientation of the TAV itself, leads to an important factor related to the enhancement of thrombosis leading to leaflet mobility problems[16, 40, 41].

d- Sinus washout

The tilt away from the sinus yielded the slowest washout and the greatly reduced velocity and vorticity for this case clearly support and explain this result. It is clear that when the SAPIEN is tilted towards the sinus, a total washout is achieved within 2 cycles faster than that with the untilted case. As explained in the shear stress section, the flow still retains more momentum compared with when it is projected downwards[39]. Thus it has a greater influence on the particle flow inside the sinus potentially increasing washout[39]. In addition, when the SAPIEN was untilted and tilted away from the sinus, the washout follows a “stair step” decay indicating that most of the initial particles that leave the sinus stay together and exit together. When the SAPIEN is tilted towards the sinus, it appears that washout is quick and characterized by intense episodes of blood change.

e- TAV angular tilts and thrombus locations

The clinical significance of the above results and discussion is clearly in the context of leaflet thrombosis post-TAVR. The development of thrombus post-TAVR is an intriguing adverse effect given the diversity of reasons that may contribute to it. It is clear that flow stasis is what aids the formation of thrombus and that it is dependent on a variety of factors such as coronary flow[16, 22, 40], valve type[13, 16], valve positioning[22] etc. Interestingly however, given that most leaflet thrombosis occurs on one or two leaflets only, it is intriguing to investigate the asymmetry in flow stasis due to potential tilt in the axis of the TAV. The patients who presented this adverse effect (Fig. 1) had their TAVs oriented at an angle with respect to the axis of the aorta. To the best of our knowledge, we have for the first time preliminarily provided data that may correlate the TAV angle tilted as discussed in the previous sections above with the alteration of shear stress distribution near the leaflets, sinus flow propagation, and significantly impacts sinus washout. Eventually, if the valve is tilted away from one sinus, it is thus tilted towards one of the 2 other sinuses. So the effect of the tilting can be extrapolated to the whole sinus-system through adding all the effects together, and the relationship with flow stasis depends on how the valve is positioned with respect to each sinus. In-vivo data show that one leaflet always has more thrombus than another and the way the valve is deployed with respect to the cusp can have an effect on that. Almost all the cases visualized in Makkar et al[6] have thrombosis on the side the TAV was pointing away corresponding to the downward tilt case presented in this paper. Future clinical studies need to be conducted to investigate tilt as a potential predictor of thrombosis as well as establish thresholds for tolerance to help in identifying appropriate follow up.

Limitations

A few limitations were present in this study. 2D fluid mechanics analysis may not be sufficient to comprehensively evaluate the flow feature in the sinus and further more elaborate experimental and computational studies are needed to investigate these flow features in more details.

Conclusion

Some patient cases with leaflet thrombosis presented angular tilts of the TAVs relative to the aortic root axis. This study constitutes a detailed look at aortic sinus hemodynamics as regulated by different angular tilts of the TAV. Novel methodology was developed to simulate *in-vitro* conditions through usage of a patient-specific 3D printed aortic valve root. Sinus flow patterns were greatly altered with the introduction of the TAV tilt compared with the untilted case. While changes in valve performance with tilt was clinically insignificant (in terms of pressure gradients), sinus vortex formation and propagation mechanisms were significantly altered. Peak sinus flow velocities and vorticities were reduced. During systole, a drastic decrease in shear stress value range and favorable probabilities (high probabilities for high shear stress) were obtained. Sinus washout was modified with the tilts. Tilting the TAV with respect to the axis of the aorta may be considered an additional factor to the list of factors that could potentially influence the risk of leaflet thrombosis.

Acknowledgment

The research done was partly supported by National Institutes of Health (NIH) under Award Number R01HL119824.

References

1. Gilard M, Eltchaninoff H, Iung B, Donzeau-Gouge P, Chevreul K, Fajadet J, Leprince P, Leguerrier A, Lievre M and Prat A. Registry of transcatheter aortic-valve implantation in high-risk patients. New England Journal of Medicine. 2012;366:1705–1715. [PubMed: 22551129]
2. Dasi LP, Hatoum H, Kheradvar A, Zareian R, Alavi SH, Sun W, Martin C, Pham T, Wang Q and Midha PA. On the mechanics of transcatheter aortic valve replacement. Annals of biomedical engineering. 2017;45:310–331. [PubMed: 27873034]
3. Lerakis S, Hayek SS and Douglas PS. Paravalvular aortic leak after transcatheter aortic valve replacement. Circulation. 2013;127:397–407. [PubMed: 23339094]
4. Klotz S, Scharfschwerdt M, Richardt D and Sievers HH. Failed valve-in-valve transcatheter aortic valve implantation. JACC: Cardiovascular Interventions. 2012;5:591–592. [PubMed: 22625200]
5. Chakravarty T, Søndergaard L, Friedman J, De Backer O, Berman D, Kofoed KF, Jilaihawi H, Shiota T, Abramowitz Y and Jørgensen TH. Subclinical leaflet thrombosis in surgical and transcatheter bioprosthetic aortic valves: an observational study. The Lancet. 2017.
6. Makkar RR, Fontana G, Jilaihawi H, Chakravarty T, Kofoed KF, De Backer O, Asch FM, Ruiz CE, Olsen NT and Trento A. Possible subclinical leaflet thrombosis in bioprosthetic aortic valves. New England Journal of Medicine. 2015;373:2015–2024. [PubMed: 26436963]
7. Yanagisawa R, Hayashida K, Yamada Y, Tanaka M, Yashima F, Inohara T, Arai T, Kawakami T, Maekawa Y and Tsuruta H. Incidence, predictors, and mid-term outcomes of possible leaflet thrombosis after TAVR. JACC: Cardiovascular Imaging. 2017;10:1–11.
8. Mangione FM, Jatene T, Gonçalves A, Fishbein GA, Mitchell RN, Pelletier MP, Kaneko T, Shah PB, Nyman CB and Shook D. Leaflet thrombosis in surgically explanted or post-mortem TAVR valves. JACC: Cardiovascular Imaging. 2017;1:82–85.
9. Toggweiler S, Schmidt K, Paul M, Cuculi F, Kobza R and Jamshidi P. Valve thrombosis 3 years after transcatheter aortic valve implantation. International journal of cardiology. 2016;207:122–124. [PubMed: 26800132]
10. Trantalis G, Toutouzas K, Latsios G, Synetos A, Brili S, Logitsi D, Penesopoulou V and Tousoulis D. TAVR and Thrombosis. JACC: Cardiovascular Imaging. 2017;10:86–87. [PubMed: 28057223]
11. Maragiannis D, Jackson MS, Igo SR, Schutt RC, Connell P, Grande-Allen J, Barker CM, Chang SM, Reardon MJ and Zoghbi WA. Replicating Patient-Specific Severe Aortic Valve Stenosis With Functional 3D ModelingCLINICAL PERSPECTIVE. Circulation: Cardiovascular Imaging. 2015;8:e003626. [PubMed: 26450122]
12. Hatoum H, Yousefi A, Lilly S, Maureira P, Crestanello J and Dasi LP. An In-Vitro Evaluation of Turbulence after Transcatheter Aortic Valve Implantation. The Journal of Thoracic and Cardiovascular Surgery. 2018.
13. Hatoum H, Dollery J, Lilly SM, Crestanello J and Dasi LP. Impact of Patient Morphologies on Sinus Flow Stasis in Transcatheter Aortic Valve Replacement: An in-vitro study. The Journal of Thoracic and Cardiovascular Surgery. 2018.
14. Kasel AM, Cassese S, Bleiziffer S, Amaki M, Hahn RT, Kastrati A and Sengupta PP. Standardized imaging for aortic annular sizing. JACC: Cardiovascular Imaging. 2013;6:249–262. [PubMed: 23489539]
15. Forleo M and Dasi LP. Effect of hypertension on the closing dynamics and lagrangian blood damage index measure of the B-Datum Regurgitant Jet in a bileaflet mechanical heart valve. Annals of biomedical engineering. 2014;42:110–122. [PubMed: 23975384]
16. Hatoum H, Moore BL, Maureira P, Dollery J, Crestanello JA and Dasi LP. Aortic sinus flow stasis likely in valve-in-valve transcatheter aortic valve implantation. The Journal of Thoracic and Cardiovascular Surgery.

17. Hatoum H, Dollery J, Lilly SM, Crestanello JA and Dasi LP. Implantation Depth and Rotational Orientation Effect on Valve-in-Valve Hemodynamics and Sinus Flow. The Annals of thoracic surgery. 2018.
18. Hatoum H, Dollery J, Lilly SM, Crestanello JA and Dasi LP. Effect of severe bioprosthetic valve tissue ingrowth and inflow calcification on valve-in-valve performance. Journal of biomechanics. 2018;74:171–179. [PubMed: 29753455]
19. Hatoum H, Heim F and Dasi LP. Stented valve dynamic behavior induced by polyester fiber leaflet material in transcatheter aortic valve devices. Journal of the Mechanical Behavior of Biomedical Materials. 2018.
20. Hatoum H, Moore BL and Dasi LP. On the Significance of Systolic Flow Waveform on Aortic Valve Energy Loss. Annals of biomedical engineering. 2018.
21. Moore BL and Dasi LP. Coronary flow impacts aortic leaflet mechanics and aortic sinus hemodynamics. Annals of biomedical engineering. 2015;43:2231–2241. [PubMed: 25636598]
22. Hatoum H, Dollery J, Lilly SM, Crestanello JA and Dasi LP. Implantation Depth and Rotational Orientation Effect on Valve-in-Valve Hemodynamics and Sinus Flow. The Annals of Thoracic Surgery.
23. Hatoum H, Moore BL, Maureira P, Dollery J, Crestanello JA and Dasi LP. Aortic sinus flow stasis likely in valve-in-valve transcatheter aortic valve implantation. The Journal of thoracic and cardiovascular surgery. 2017;154:32–43. e1. [PubMed: 28433356]
24. Midha PA, Raghav V, Okafor I and Yoganathan AP. The Effect of Valve-in-Valve Implantation Height on Sinus Flow. Annals of biomedical engineering. 2016:1–8. [PubMed: 26620776]
25. Vahidkhah K and Azadani AN. Supra-annular Valve-in-Valve implantation reduces blood stasis on the transcatheter aortic valve leaflets. Journal of Biomechanics. 2017;58:114–122. [PubMed: 28511838]
26. Kumar G, Raghav V, Lerakis S and Yoganathan AP. High Transcatheter Valve Replacement May Reduce Washout in the Aortic Sinuses: an In-Vitro Study. The Journal of heart valve disease. 2015;24:22–29. [PubMed: 26182616]
27. Dhanak M and Bernardinis BD. The evolution of an elliptic vortex ring. Journal of Fluid Mechanics. 1981;109:189–216.
28. Didden N On the formation of vortex rings: rolling-up and production of circulation. Zeitschrift für Angewandte Mathematik und Physik (ZAMP). 1979;30:101–116.
29. Peacock JA. An in vitro study of the onset of turbulence in the sinus of Valsalva. Circulation research. 1990;67:448–460. [PubMed: 2376081]
30. Walker J, Smith C, Cerra A and Doligalski T. The impact of a vortex ring on a wall. Journal of Fluid Mechanics. 1987;181:99–140.
31. Chandra S, Rajamannan NM and Sucosky P. Computational assessment of bicuspid aortic valve wall-shear stress: implications for calcific aortic valve disease. Biomechanics and modeling in mechanobiology. 2012;11:1085–1096. [PubMed: 22294208]
32. Yap CH, Liu X and Pekkan K. Characterizaton of the vessel geometry, flow mechanics and wall shear stress in the great arteries of wildtype prenatal mouse. PloS one. 2014;9:e86878. [PubMed: 24475188]
33. Traub O and Berk BC. Laminar shear stress: mechanisms by which endothelial cells transduce an atheroprotective force. Arteriosclerosis, thrombosis, and vascular biology. 1998;18:677–685.
34. Berk BC, ABE JI, Min W, Surapisitchat J and Yan C Endothelial atheroprotective and anti-inflammatory mechanisms. Annals of the New York Academy of Sciences. 2001;947:93–111. [PubMed: 11795313]
35. Wu M, Kouchi Y, Onuki Y, Shi Q, Yoshida H, Kaplan S, Viggers RF, Ghali R and Sauvage LR. Effect of differential shear stress on platelet aggregation, surface thrombosis, and endothelialization of bilateral carotid-femoral grafts in the dog. Journal of vascular surgery. 1995;22:382–90; discussion 390–2. [PubMed: 7563399]
36. Cunningham KS and Gotlieb AI. The role of shear stress in the pathogenesis of atherosclerosis. Laboratory investigation. 2005;85:9. [PubMed: 15568038]

37. Saw SN, Dawn C, Biswas A, Mattar CNZ and Yap CH. Characterization of the in vivo wall shear stress environment of human fetus umbilical arteries and veins. Biomechanics and modeling in mechanobiology. 2017;16:197–211. [PubMed: 27456489]

38. Casa LD, Deaton DH and Ku DN. Role of high shear rate in thrombosis. Journal of vascular surgery. 2015;61:1068–1080. [PubMed: 25704412]

39. Mittal R, Rampunggoon P and Udaykumar H. Interaction of a synthetic jet with a flat plate boundary layer. AIAA paper. 2001;2773:1.

40. Hatoum H, Crestanello JA and Dasi LP. Possible Subclinical Leaflet Thrombosis in Bioprosthetic Aortic Valves. New England Journal of Medicine. 2016;374:1591–1591.

41. Bark DL, Para AN and Ku DN. Correlation of thrombosis growth rate to pathological wall shear rate during platelet accumulation. Biotechnology and bioengineering. 2012;109:2642–2650. [PubMed: 22539078]

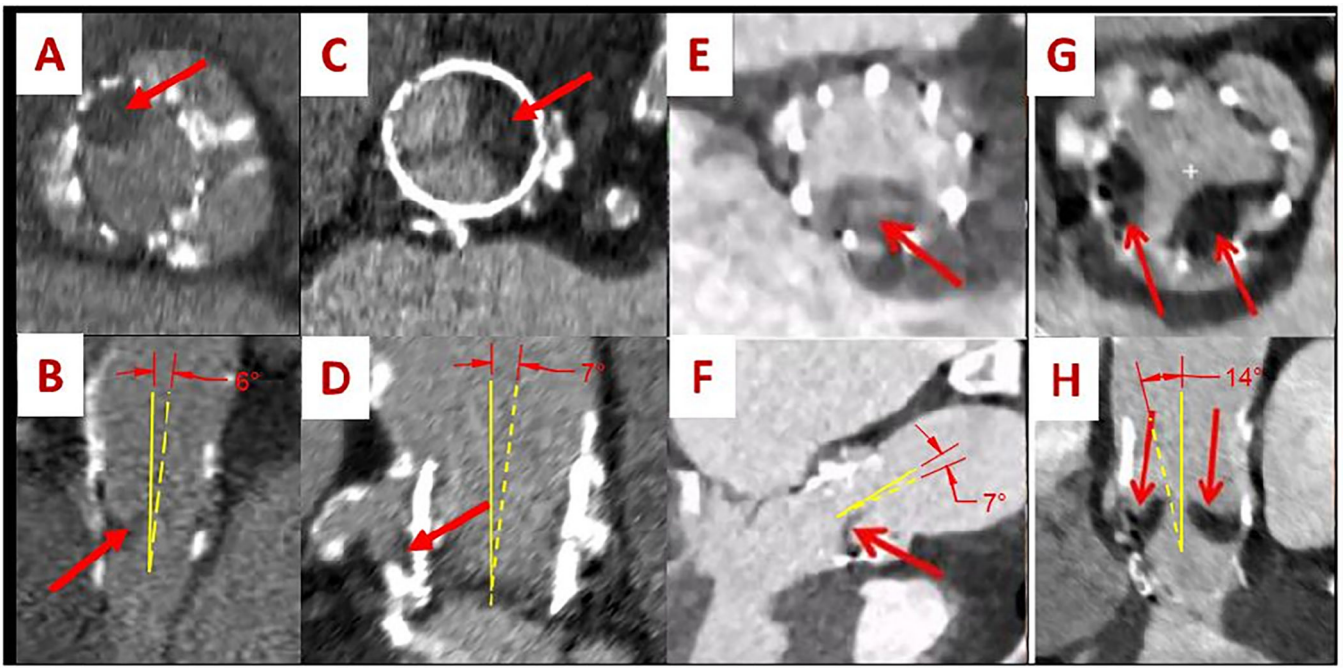

Figure 1:
CT images of 4 different patients with leaflet thrombosis showing the relative position of the thrombus on the leaflets (A, C, E and G) along with the tilted orientation of the TAV with respect to the axis of the aorta (B, D, F and H). The red arrows point out at the thrombus. The yellow dashed lines represent the axis of the implanted TAV and the full yellow lines represent the axis of the aorta. Figures E, F, G and H are taken from Ref[6] with permission.

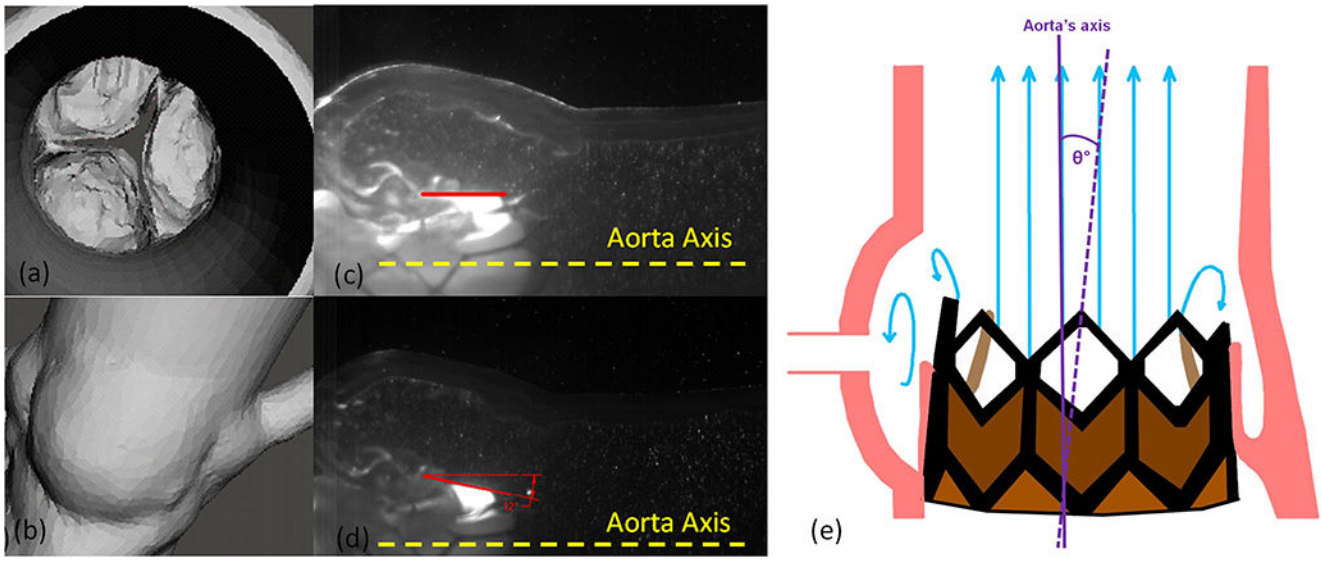

Figure 2:

(a) Aortic and (b) Sinus view of the segmented valve and Valve placement view with respect to the aorta axis (a) untilted and (b) tilted away from the sinus.

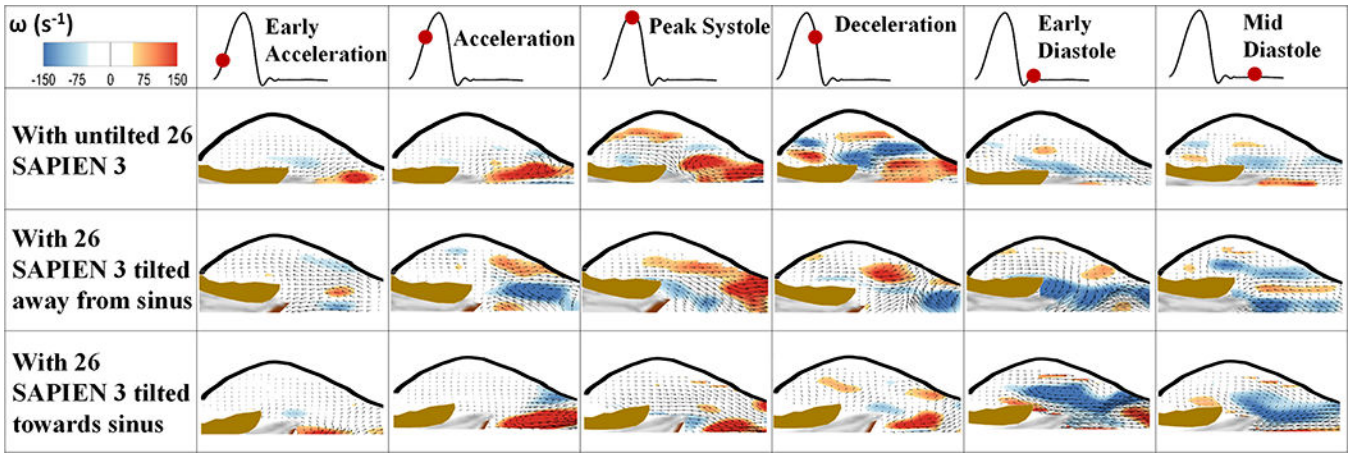

Figure 3:

Velocity vectors and vorticity contours within the sinus of an aortic valve post-TAVR with Sapien S3 26 untilted and tilted away from the sinus and towards sinus at selected time points throughout the cardiac cycle.

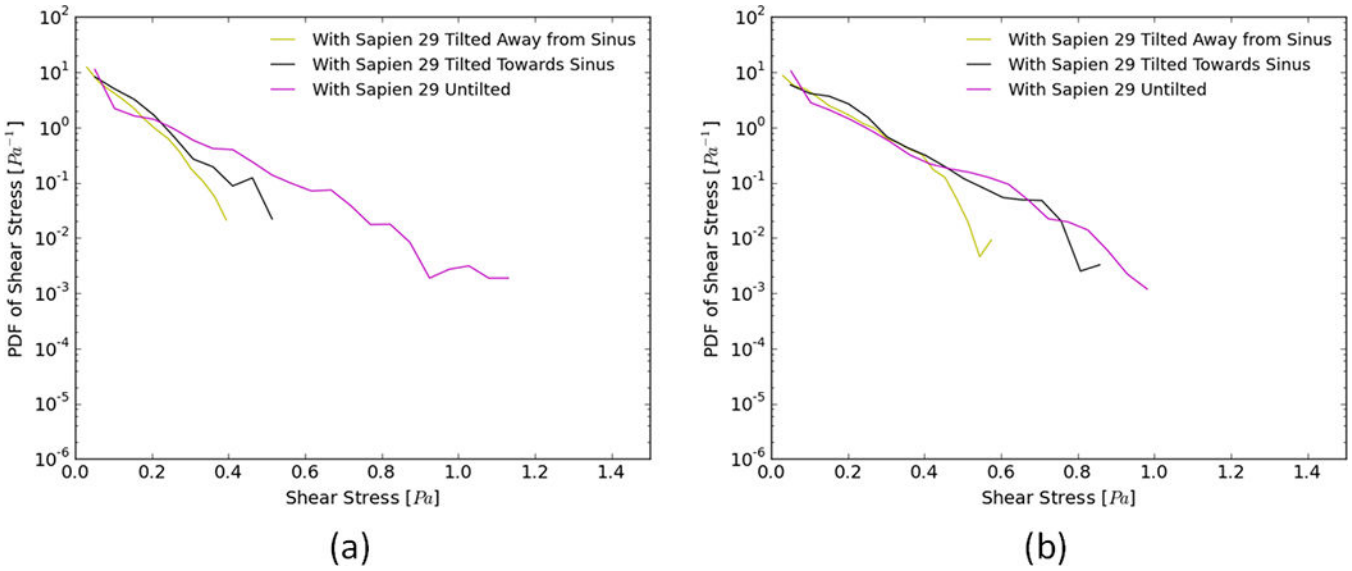

Figure 4a and b:

Probability density function in log scale of varying shear stress distribution values along a sub-region near the valve leaflets during (a) systole and (b) diastole for different valve configurations.

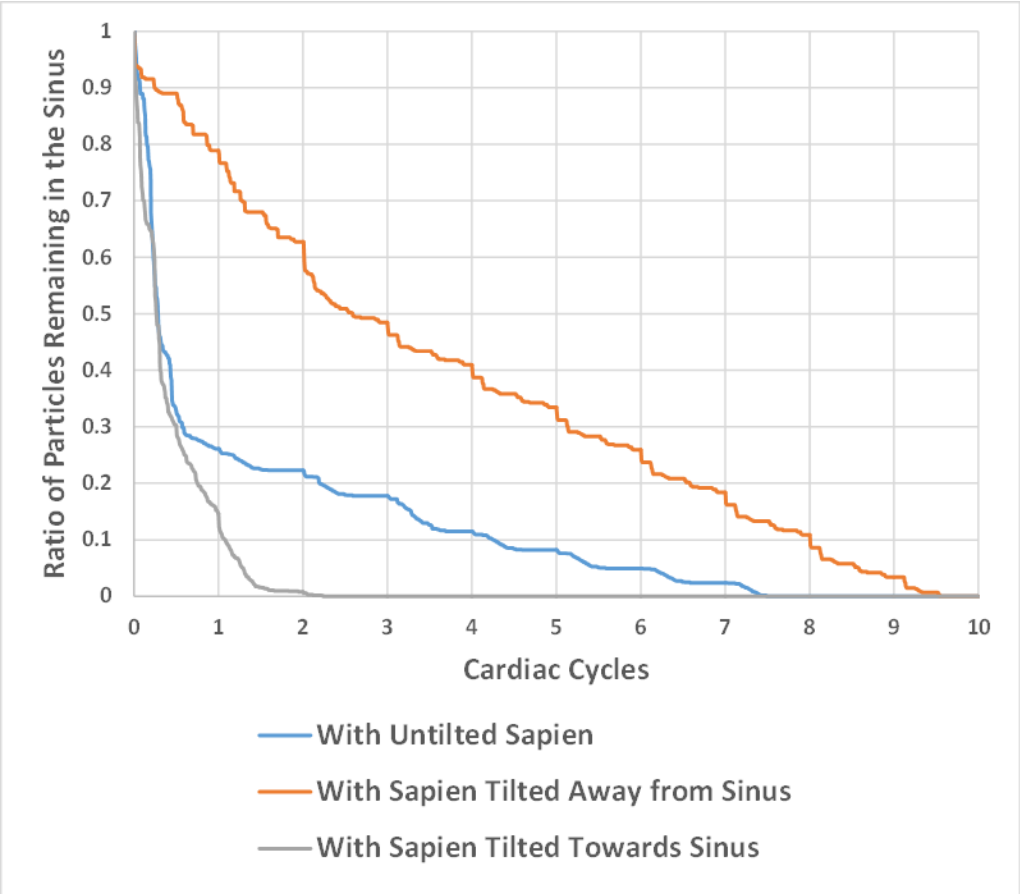

Figure 5:
Survival probability curve of particles remaining in the sinus of the bicuspid and tricuspid valves with different valve configurations.

Table 1:

Hemodynamic parameters of the valve with the different TAV orientations. CO denotes the cardiac output and ΔP the average pressure gradient.

	With Untilted Sapien S3 26	With tilted Sapien S3 26 away from sinus	With tilted Sapien S3 26 towards sinus
CO (L/min)	5.3	5.3	5.3
Heart Rate (BPM)	81	81	81
ΔP (mmHg)	20.14±0.16	17.71±0.77	15.32±0.33